

Breathing dynamics of dissipative pure quartic soliton molecules via spectral filtering effects

Chun-Ting Liu(刘春廷), Jun-You Lu(卢俊佑), Han-Yang Shen(申翰阳), and Zu-Xing Zhang(张祖兴)
Citation: Chin. Phys. B, 2026, 35 (**3**): 034205. DOI: 10.1088/1674-1056/adf1eb
http://cpb.iphy.ac.cn; http://iopscience.iop.org/cpb

What follows is a list of articles you may be interested in

Chaotic dynamics of Pr^{3+}/Yb^{3+}-doped all-fiber up-conversion visible fiber laser

Yisong Li(李义松), Yueling Hao(郝悦伶), Juanfen Wang(王娟芬), Xiaohui Chen(陈晓晖), Shengxiang Chen(陈胜祥), Chao Zhou(周超), and Lingzhen Yang(杨玲珍)
Chin. Phys. B, 2026, 35 (**1**): 014208. DOI: 10.1088/1674-1056/ade4b5

Pure-quartic soliton molecules in normal fourth-order dispersion regimes based on spectral filtering effect

Han-Yang Shen(申翰阳), Rui-Bo Lan(蓝睿博), Hong-Bin Hu(胡洪彬), Yang Li(李阳), Rui Zhou(周瑞), and Zu-Xing Zhang(张祖兴)
Chin. Phys. B, 2025, 34 (**3**): 034203. DOI: 10.1088/1674-1056/ada43c

Femtosecond mode-locking and soliton molecule generation based on a GaAs saturable absorber

Chen-Yan Zhang(张辰妍), Xin-He Dou(窦鑫河), Zhen Chen(陈震), Jing-Han Zhao(赵靖涵), Wei Sun(孙薇), Ze-Yu Fan(樊泽宇), Tao Zhang(张涛), Hao Teng(滕浩), and Zhi-Guo Lv(吕志国)
Chin. Phys. B, 2025, 34 (**1**): 014205. DOI: 10.1088/1674-1056/ad8db3

Real-time observation of soliton pulsation in net normal-dispersion dissipative soliton fiber laser

Xu-De Wang(汪徐德), Xu Geng(耿旭), Jie-Yu Pan(潘婕妤), Meng-Qiu Sun(孙梦秋), Meng-Xiang Lu(陆梦想), Kai-Xin Li(李凯芯), and Su-Wen Li(李素文)
Chin. Phys. B, 2023, 32 (**2**): 024210. DOI: 10.1088/1674-1056/ac76b0

Generation of breathing solitons in the propagation and interactions of Airy-Gaussian beams in a cubic-quintic nonlinear medium

Weijun Chen(陈卫军), Ying Ju(鞠莹), Chunyang Liu(刘春阳), Liankai Wang(王连锴), Keqing Lu(卢克清)
Chin. Phys. B, 2018, 27 (**11**): 114216. DOI: 10.1088/1674-1056/27/11/114216

Breathing dynamics of dissipative pure quartic soliton molecules via spectral filtering effects

Chun-Ting Liu(刘春廷), Jun-You Lu(卢俊佑), Han-Yang Shen(申翰阳), and Zu-Xing Zhang(张祖兴)†

Advanced Photonic Technology Laboratory, College of Electronic and Optical Engineering & College of Flexible Electronics (Future Technology), Nanjing University of Posts and Telecommunications, Nanjing 210023, *China*

(Received 28 May 2025; revised manuscript received 14 July 2025; accepted manuscript online 19 July 2025)

Although dissipative pure quartic solitons (DPQSs) stabilized by fourth-order dispersion (FOD) and nonlinearity are widely studied, their multi-soliton dynamics in positive FOD remain underexplored. Here, we study the impact of saturation energy and filter bandwidth on breathing DPQS molecules numerically. Our findings indicate that complementary breathing DPQS molecules exchange energy through oscillating tails, exhibiting simultaneously temporal oscillations and spectral shifting. By adjusting cavity parameters, we demonstrate that the state of breathing soliton molecules is inherently governed by time separation. These findings deepen the comprehension of multi-soliton interactions and nonlinear phenomena.

Keywords: dissipative pure-quartic soliton, soliton molecule, breathing soliton, oscillating tails

PACS: 42.65.Sf, 42.65.Tg, 42.55.Wd, 42.60.Fc

DOI: 10.1088/1674-1056/adf1eb **CSTR:** 32038.14.CPB.adf1eb

1. Introduction

Solitons, a unique type of nonlinear localized waves,[1] have attracted considerable research attention due to their exceptional stability and ability to propagate over long distances without distortion.[2] Over subsequent decades, soliton phenomena have been observed across diverse fields, including quantum fluids,[3,4] microcavity optics,[5,6] and laser physics.[7,8] Their remarkable application prospects have driven development across multiple areas, particularly in quantum information processing,[9] optical frequency combs,[10,11] and fiber-optic communications.[12] Solitons are also ubiquitously observed in non-conservative systems. In nonlinear optical systems, localized waves formed through the balanced interplay of gain, loss, dispersion, and nonlinear effects are formally designated as dissipative solitons.[13–15]

Passively mode-locked fiber lasers (PMFL) have emerged as an ideal platform for investigating nonlinear dissipative dynamics.[16,17] When configured to operate within a dissipative regime, PMFL generates optical dissipative solitons that exhibit rich nonlinear phenomena under specific conditions, including breathing soliton,[18–20] soliton pulsation,[21–25] and soliton explosions.[26–29] Traditional investigations have predominantly characterized higher-order dispersion as a detrimental factor because it induces soliton distortion and energy dissipation. Consequently, prior studies of optical soliton dynamics have primarily focused on second-order dispersion (SOD) regimes under dispersion management, with limited exploration of higher-order dispersion effects. However, a shift occurred with the experimental discovery of pure-quartic solitons (PQSs) governed by fourth-order dispersion (FOD) in 2016.[30–33] Subsequently, PQS shows an inverse cubic relationship between energy and pulse width,[34] surpassing the picojoule-level energy constraints characteristic of traditional solitons. This breakthrough has since triggered comprehensive investigations into quartic soliton dynamics.

Multiple soliton formation constitutes a prevalent phenomenon in PMFL. Under elevated pump power conditions, energy accumulation causes soliton splitting. In contrast, PQS molecules exhibit stability characteristics. Their oscillatory tails effectively establish a potential barrier that induces repulsive forces between adjacent solitons, thereby enhancing robustness against perturbations and significantly inhibiting fission processes.[35] The realization of stable multi-soliton states under net normal FOD conditions is unresolved. Current research on PQS molecules has mostly been conducted exclusively in net anomalous FOD regimes,[36] Recently, Shen *et al*. innovatively leveraged spectral filtering effects to lower the threshold for pulse splitting.[37] This finding enables the exploration of multi-soliton nonlinear dynamics in normal FOD regions.

In this work, we numerically and comprehensively study breathing soliton molecules in a normal FOD fiber laser and uncover a special breathing mode, which is, DPQS molecules exhibit a complementary breathing mode. That is because oscillating tails serving as the channel for energy transfer connect different solitons, enabling energy exchange between these solitons. Moreover, we demonstrate that the separation affects the interaction between different solitons, changing the breathing mode. More interestingly, the oscillating tails exhibit creeping when energy is transferred through them. These

†Corresponding author. E-mail: zxzhang@njupt.edu.cn

© 2026 Chinese Physical Society and IOP Publishing Ltd. All rights, including for text and data mining, AI training, and similar technologies, are reserved.

discoveries advance the understanding of multi-soliton nonlinear dynamics in dissipative optical systems.

2. Numerical method

Our numerical model employs a PMFL configuration, schematically illustrated in Fig. 1(a). The laser cavity consists of a spectral pulse shaper (SPS), Er-doped fibers (EDFs), a saturable absorber (SA), a spectral filter, single-mode fibers (SMFs), and an output coupler (OC). The nonlinear Schrödinger equation (NLSE) is used to describe the propagation dynamics of solitons, which is classically of the form

$$\frac{\partial A}{\partial z} = -\frac{\mathrm{i}\beta_2}{2}\frac{\partial^2 A}{\partial t^2} + \frac{\beta_3}{6}\frac{\partial^3 A}{\partial t^3} + \frac{\mathrm{i}\beta_4}{24}\frac{\partial^4 A}{\partial t^4} + \mathrm{i}\gamma|A|^2 A + \frac{g-\alpha}{2}A, \tag{1}$$

where A, t, γ, and z respectively represent the slowly varying amplitude of the pulse envelope, the temporal coordinate, the nonlinear coefficient, and the propagation distance. β_2, β_3, and β_4 denote the fiber's second-order dispersion (SOD), third-order dispersion (TOD), and FOD of the fiber. Within the EDFs, α and g correspond to the loss and gain coefficients, respectively. Where the g of the EDF is defined as

$$g = \frac{g_0}{1 + \int |A(z,t)|^2 \,\mathrm{d}t / E_{\mathrm{sat}} + \left(\omega/\Omega_{\mathrm{g}}\right)^2}, \tag{2}$$

where g_0 is the small-signal gain coefficient, ω is angular frequency, E_{sat} and Ω_{g} denote saturation energy and gain bandwidth of the EDF. The SA, which is related to the pulse intensity, can be described as

$$T = 1 - \frac{q_0}{1 + |A(z,t)|^2 / P_{\mathrm{sat}}}, \tag{3}$$

where q_0 and P_{sat} represent the modulation depth and saturation power of the SA, respectively. The SPS generates a customizable phase distribution, and the phase modulation function of SPS on propagating pulse can be written as

$$\phi(\omega) = \beta_2\frac{(\omega-\omega_0)^2}{2} + \beta_3\frac{(\omega-\omega_0)^3}{6} + \beta_4\frac{(\omega-\omega_0)^4}{24}. \tag{4}$$

Here, ω_0 represent the central angular frequency. A Lorentzian filter is added into the cavity, with its transfer function can be expressed as

$$F(\omega) = \frac{1}{1 + [(\omega-\omega_0)/\Delta\omega]^2}, \tag{5}$$

where $\Delta\omega$ is the filter bandwidth expressed in angular frequency. The central wavelength of the Lorentzian filter operates is 1550 nm and $\Delta\omega$ is set to 5 ps^{-1}.

The initial simulation parameters are listed in Table 1. The seed signal is a relatively weak pulse, it propagates through: EDF → SA → filter → OC → SPS. All components are connected with SMF. The total fiber's SOD $\beta_2 = 0.032$ ps^2, TOD $\beta_3 = 0$ ps^3, and FOD $\beta_4 = -0.0000044$ ps^4. We use SPS to manage the dispersion of the fiber laser. The SPS serves two aims; to compensate the SOD and TOD by optical fibers, so that net cavity dispersion of these orders is negligible,[34] as illustrated in Fig. 1(b); and introduce FOD values of 0.47 ps^4, which dominates the propagation, as shown in Fig. 1(c). The NLSE is solved numerically by the split-step Fourier method, and temporal and spectral information are recorded during propagation through the OC for each roundtrip (RT).

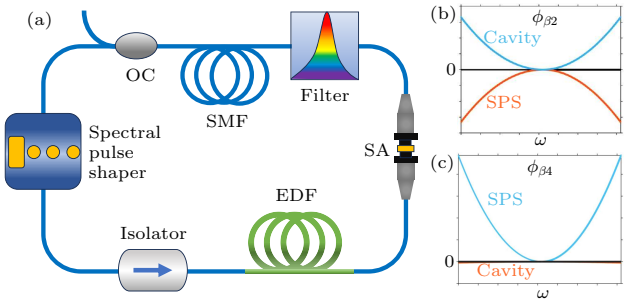


Fig. 1. Principle of operation of the laser. (a) Schematic diagram of the fiber laser used for simulation. (b) Quadratic and (c) quartic dispersive phase imparted by the cavity and the spectral pulse shaper.

Table 1. Initial component parameters.

Element	Parameter	Value
EDF	length	2 m
	$\beta_{2-\mathrm{EDF}}$	60 ps^2/km
	$\beta_{3-\mathrm{EDF}}$	0 ps^3/km
	$\beta_{4-\mathrm{EDF}}$	0.0022 ps^4/km
	γ_{EDF}	0.006 W^{-1}·m^{-1}
	g_0	1.5 m^{-1}
	E_{sat}	70 pJ
	Ω_{g}	30 nm
SMF	length	4 m
	$\beta_{2-\mathrm{SMF}}$	−22 ps^2/km
	$\beta_{3-\mathrm{SMF}}$	0 ps^3/km
	$\beta_{4-\mathrm{SMF}}$	−0.0022 ps^4/km
	γ_{SMF}	0.0015 W^{-1}·m^{-1}
SA	q_0	0.4
	P_{sat}	50 W
Filter	$\Delta\omega$	5 ps^{-1}
SPS	β_2	−0.032 ps^2
	β_3	0 ps^3
	β_4	0.4700044 ps^4

3. Results and analysis

3.1. Breathing single DPQS

The formation of DPQS is essentially governed by the modulation instability (MI) dynamics. Specifically, the chaotic, stable, and breathing states of DPQS correspond respectively to the MI system residing in an unmodulated continuous-wave (CW) state, a cosine-modulated state, and a transitional state between the CW state and the cosine-modulated state.[38]

In the non-stationary propagation scenarios, the nonlinear localized structures exhibiting periodic energy evolution are vividly termed as breathing or pulsating solitons.[39] In simulations, the pump power is linked with E_{sat}. When E_{sat} is set to 70 pJ, the laser outputs breathing single DPQS, as displayed in Fig. 2. Figures 2(a) and 2(b) illustrate the temporal and spectral evolutions over 600 RTs, respectively, as they exhibit the typical breathing features of oscillating propagation in time, spectral, and energy.[39] To better characterize breathing DPQS, the single-shot time and spectral profile at 550 RT is fetched. In Fig. 2(c), the chirp of breathing DPQS increases linearly in the center of the pulse. The corresponding spectra display similar characteristics under the linear and logarithmic coordinates, i.e., the intensity obviously dropped in the center, as depicted in Fig. 2(d). The DPQS exhibits oscillating tails in temporal profile, primarily owing to higher optical power disrupting the phase-matching relationship between the main lobe of DPQS and temporal pedestals. This disruption subsequently triggers periodic energy redistribution across the whole pulse profile, ultimately facilitating sustained energy exchange between the main lobe and pedestal.[25,40]

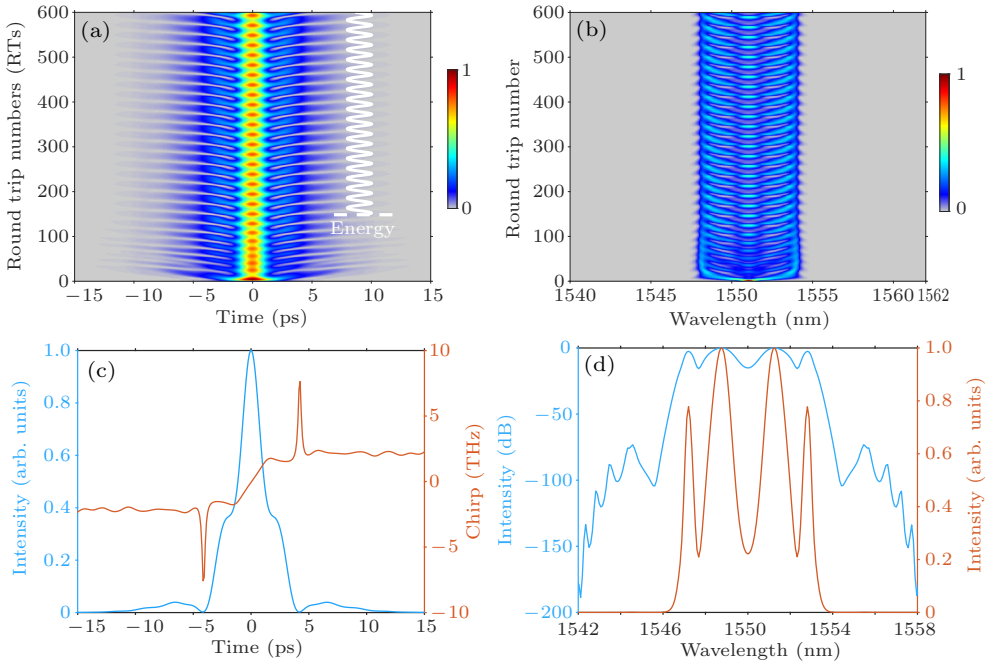


Fig. 2. Breathing DPQS. (a) Temporal and (b) spectral evolution over 600 RTs. Inset of (a): energy evolution; single-shot (c) time and (d) spectral profile under the 550th RT.

3.2. Breathing DPQS molecules containing two solitons

To get the breathing DPQS molecules containing two solitons, reducing the filter bandwidth to provide more spectral loss is necessary, which lowers the splitting threshold.[37] When saturation energy is elevated, it could disrupt the relative equilibrium between two solitons, triggering periodic energy exchange and exhibiting breathing dynamics. We set the E_{sat} to 85 pJ and the filter bandwidth $\Delta\omega$ to 4 ps^{-1}. As shown in Fig. 3(a), soliton 1 and soliton 2 exhibit complementary breathing patterns, with oscillating tails simultaneously demonstrating a creeping-like shift. The soliton interaction shows a complementary relationship, when soliton 1 reaches the maximum energy, soliton 2 reaches the minimum energy, and conversely, aligning with certain reports.[41] Breathing soliton molecules exhibit complementary intensity variations due to their mutual interaction, which have some connections to generalized beating-like dynamics. However, two primary distinctions of breathing soliton and beating soliton exist: (i) Beating solitons display complementary intensity changes between components with distinct directions,[42] whereas in our study, the breathing soliton molecules show complementary intensity changes from interactions between two solitons. (ii) The total intensity of a single beating soliton remains stable,[42] whereas that of a breathing soliton experiences periodic oscillations. This oscillation with a period of approximately 280 RTs, this periodic pattern is further corroborated by the energy evolution in the insets of Fig. 3(a). Because of the interactions between soliton 1 and soliton 2, oscillating tails shift periodically, manifesting as a creeping dynamic with a 280 RTs periodicity. This shifting exhibits more stronger creeping amplitude relative to previous studies.[36] Additionally, the spectral evolution in Fig. 3(b) reveals that weak interference spectral components exhibit a slow wavelength shift across evolution.

To investigate the underlying mechanism of this phenomenon, we selected five typical RTs corresponding to energy extrema within one breathing period at the 700th, 770th,

840th, 910th, and 980th RT, as shown in Figs. 3(c) and 3(d). These temporal and spectral profiles reveal that the width of soliton molecules remains basically unchanged, while the oscillating tails exhibit periodic positional shifts. Simultaneously, spectral distributions reveal oscillatory lateral shifts of the central wavelength. These findings, periodic intensity modulation of the main pulse, coupled with weak trailing pulse shift in breathing soliton molecules, collectively elucidate the complementary mechanism of breathing soliton molecules in the dissipative system. The creeping behavior originates from the energy exchange between the main pulse and its oscillatory tails.

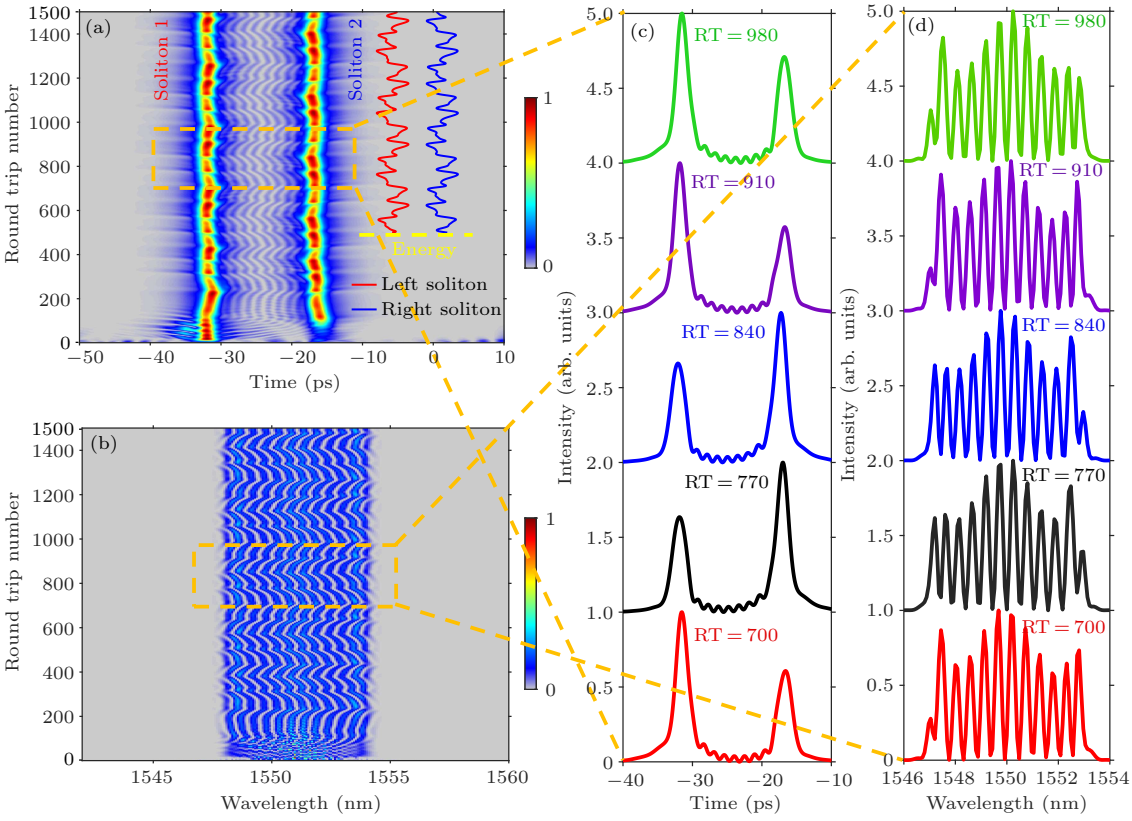


Fig. 3. Breathing DPQS molecules containing two solitons. (a) Temporal and (b) spectral evolutions over 1500 RTs. Insets of (a): the energy evolution of soliton 1 and soliton 2; (c) temporal and (d) spectral profiles at different RTs in one period.

3.3. Breathing DPQS molecules containing three solitons

The interaction behavior of the soliton molecule is influenced greatly by pulse separation.[39,43] This principle is equally applicable to DPQS molecules under normal FOD. We set E_{sat} to 95 pJ and the filter bandwidth $\Delta\omega$ to 3 ps^{-1}. Figures 4(a) and 4(c) reveal a complementary breathing mode in soliton molecules, which show energy exchanges between soliton 1, soliton 3, and soliton 2 during three soliton interactions and demonstrate that the breathing period is 92 RTs. Figure 4(d) captures the temporal evolution from 40th to 80th RT. During this process, oscillating tails as a link enable energy transfer between soliton 1, soliton 3, and soliton 2, as depicted in Fig. 4(c). This link makes synchronized intensity oscillations in soliton 1 and soliton 3. Spectral interference emerges when DPQS molecules are generated, as evidenced in Figs. 4(b) and 4(e). The typical temporal and spectral profiles in one breathing period are displayed in Figs. 4(f) and 4(g). It can be obviously seen that the energy of soliton 2 first transfers into soliton 1 and soliton 3, and then the energy will flow back into soliton 2. This complementary intensity variation is similar to the power exchange between the pump and sidebands exhibited by Akhmediev breathers (ABs) within the modulation instability (MI) system.[38]

To comprehensively investigate breathing DPQS molecules dynamics in fiber lasers, we set E_{sat} to 100 pJ and the filter bandwidth $\Delta\omega$ to 4 ps^{-1}. The temporal evolution in Fig. 5(a) reveals the dynamics of breathing DPQS molecules. The breathing period of soliton 3 is 70 RTs, while the period of soliton 1 and soliton 2 is 130 RTs, which is approximately double the period of soliton 1. For better clarity, we also provide the temporal and spectral evolution with a breathing period, as depicted in Figs. 5(c) and 5(d). It reveals that periodic energy exchange between soliton 1 and soliton 2 through oscillating tails, this process shows complementary characteristics, as displayed in the inset of Fig. 5(a). Soliton 1 and soliton 2 exhibit a creeping-like shift in oscillating tails through strong interaction because of little separation between them, while soliton 3 maintains different breathing modes owing to its larger separation from the other solitons. Spectral evolution in Figs. 5(b) and 5(d) displays breathing character-

istics in the central regions. These findings reveal that the separation of solitons can affect their interactions, which is attributed to the capability of the tails of the pulse to establish a linkage between soliton molecules and trigger energy transfer.

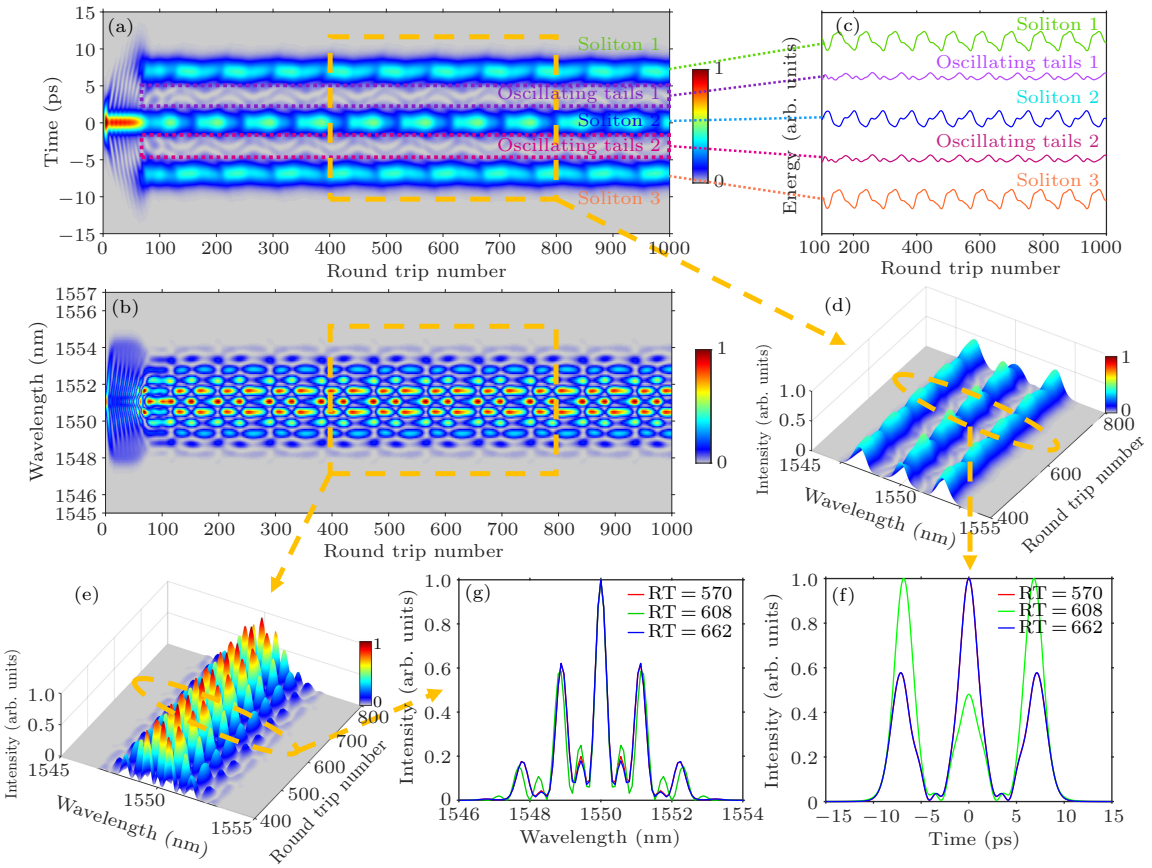


Fig. 4. Breathing DPQS molecules with strong interactions. (a) Temporal and (b) spectral evolutions for 1000 RTs; (c) the energy evolutions of soliton 1, soliton 2, soliton 3, oscillating tails 1 and oscillating tails 2; local enlargement of (d) temporal and (e) spectral evolutions from the 400 RT to 800 RT; (f) temporal and (g) spectral profiles at different RTs in one period.

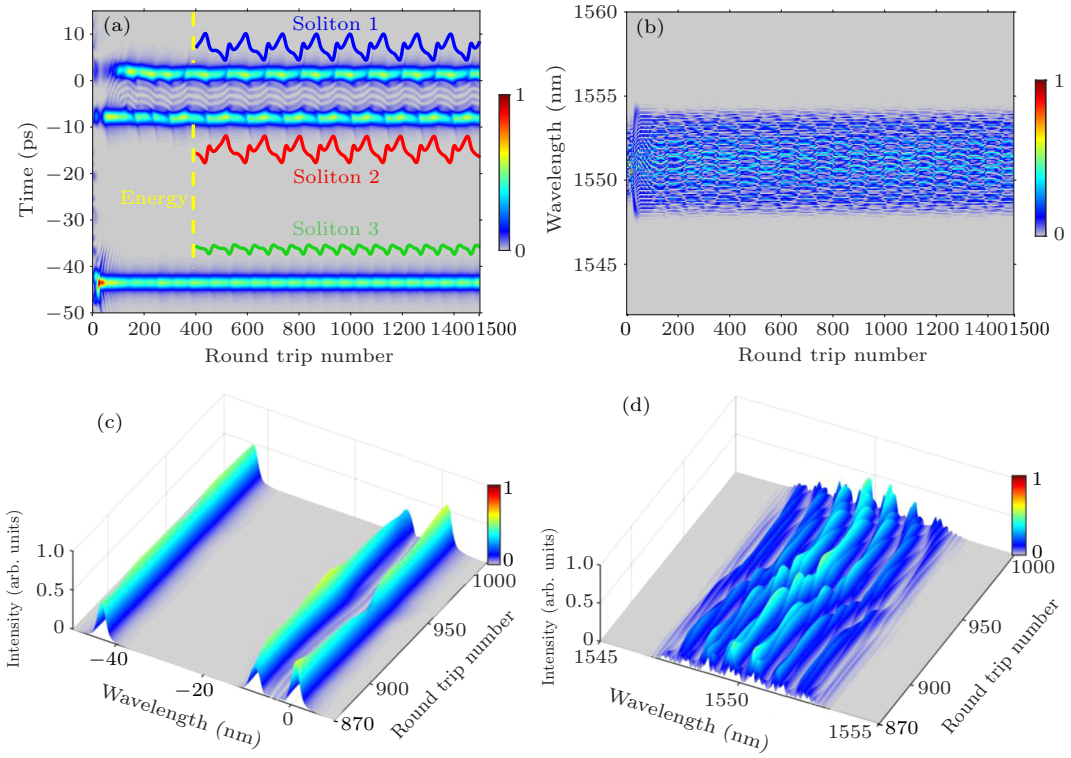


Fig. 5. Breathing DPQS molecules containing three solitons. (a) Temporal and (b) spectral evolutions for 1500 RTs. Inset of (a): the energy evolutions of soliton 1, soliton 2, and soliton 3; (c) temporal and (d) spectral evolutions for one period.

The DPQSs exhibit different states when the system parameters are modulated. It is necessary to investigate the influence of filter bandwidths $\Delta\omega$ and saturation energy $E_{\rm sat}$ on breathing DPQSs dynamics. $\Delta\omega$ provides spectral loss and $E_{\rm sat}$ drives nonlinear effects, due to both of them corresponding to the possible modulation of laser in practice, our exploration exhibits practical value for potential applications. Figure 6 presents the state distribution of DPQS under different filter bandwidths and saturation energy, where $\Delta\omega$ is incremented in 0.5 ps^{-1} steps and $E_{\rm sat}$ is incremented in 5 pJ steps. It can be found that when the filter bandwidth is in the range of 4.5 ps^{-1}–6 ps^{-1}, DPQSs are more likely to be in a single state, with the $E_{\rm sat}$ increasing, DPQSs evolve into chaos directly. This phenomenon arises from an insufficient lowering of the splitting threshold induced by spectral filtering. When the filter bandwidth is in the range of 3 ps^{-1}–4 ps^{-1}, DPQSs are more likely to split and evolve into breathing soliton molecules. With the nonlinear gain increases, DPQSs split to more solitons rather than evolve into chaos. Notably, breathing soliton molecules in positive FOD are also more likely to appear at the boundary between one stable soliton molecule region to another stable region. This suggests that when tuning parameters near the mode-locking threshold, energy began to exchange between the main lobe and pedestal of the soliton inducing tails oscillating. If the separation between solitons is small, the oscillating tails can link different solitons and facilitate energy exchange, forming complementary breathing solitons molecules.

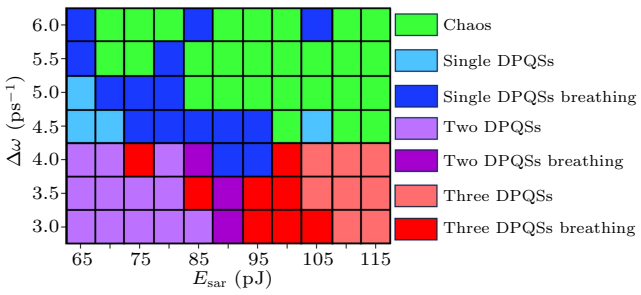


Fig. 6. State distribution under different $E_{\rm sat}$ and $\Delta\omega$.

4. Discussion and conclusion

In summary, we numerically investigated the breathing dynamics of DPQS molecules in PMFL under normal FOD with spectral filtering effects. Complex breathing phenomena emerge between multiple DPQSs when adjusting pump power and filter bandwidth. Unlike conventional PQS governed by anomalous FOD, breathing DPQS molecules under normal FOD exhibit oscillatory tails creeping and spectral shifting. The emergence of intricate breathing DPQS molecules arises due to energy exchange not only between the main lobe of the soliton and its oscillating tails but also between the two solitons, oscillatory tails acting as energy carriers. These oscillatory tails serve as energy transfer channels, being crucial for driving complementary breathing patterns and triggering creeping dynamics. Moreover, at larger soliton separation, the link between the solitons through oscillating tails is so weak that they virtually have no effect on each other, whereas closer separation enables energy transfer through oscillatory tails, interacting with each other and changing breathing periods. These findings not only offer novel insights into the breathing mechanisms of multiple DPQSs but also advance the understanding of nonlinear dynamics in multi-soliton systems.

Acknowledgement

Project supported by the National Natural Science Foundation of China (Grant No. 62175116).

References

[1] Busch T and Anglin J R 2001 *Phys. Rev. Lett.* **87** 010401
[2] Musslimani Z H, Makris K G, El-Ganainy R and Christodoulides D N 2008 *Phys. Rev. Lett.* **100** 030402
[3] Strecker K E, Partridge G B, Truscott A G and Hulet R G 2002 *Nature* **417** 150
[4] Seadawy A R 2012 *Appl. Math. Lett.* **25** 687
[5] Yi X, Yang Q F, Yang K Y, Suh M G and Vahala K 2015 *Optica* **2** 1078
[6] Herr T, Brasch V, Jost J D, Wang C Y, Kondratiev N M, Gorodetsky M L and Kippenberg T J 2014 *Nat. Photon.* **8** 145
[7] Zhang Z X, Wu J, Xu K and Lin J T 2009 *Laser Technol.* **33** 548
[8] Keller U, Weingarten K J, Kartner F X, Kopf D, Braun B, Jung I D, Fluck R, Honninger C, Matuschek N and derAu J A 1996 *IEEE J. Sel. Top. Quantum Electron.* **2** 435
[9] Lukin D M, White A D, Trivedi R, Guidry M A, Morioka N, Babin C, Soykal O O, Ul-Hassan J, Son N T, Ohshima T, Vasireddy P K, Nasr M H, Sun S, MacLean J P W, Dory C, Nanni E A, Wrachtrup J, Kaiser F and Vuckovic J 2020 *npj Quantum Inf.* **6** 80
[10] Kippenberg T J, Holzwarth R and Diddams S A 2011 *Science* **332** 555
[11] Del'Haye P, Schliesser A, Arcizet O, Wilken T, Holzwarth R and Kippenberg T J 2007 *Nature* **450** 1214
[12] Mollenauer L F, Stolen R H and Gordon J P 1980 *Phys. Rev. Lett.* **45** 1095
[13] Grelu P and Akhmediev N 2012 *Nat. Photon.* **6** 84
[14] Qian Z C, Liu M, Luo A P, Luo Z C and Xu W C 2022 *Opt. Express* **30** 22066
[15] Wang Z Q, Nithyanandan K, Coillet A, Tchofo-Dinda P and Grelu P 2019 *Nat. Commun.* **10** 830
[16] Finot C, Provost L, Petropoulos P and Richardson D J 2007 *Opt. Express* **15** 852
[17] Matsas V J, Newson T P, Richardson D J and Payne D N 1992 *Electron. Lett.* **28** 1391
[18] Peng J, Boscolo S, Zhao Z and Zeng H 2019 *Sci. Adv.* **5** eaax1110
[19] Ablowitz M J and Musslimani Z H 2013 *Phys. Rev. Lett.* **110** 064105
[20] Lucas E, Karpov M, Guo H, Gorodetsky M L and Kippenberg T J 2017 *Nat. Commun.* **8** 736
[21] Wang X, Liu Y G, Wang Z, Yue Y, He J, Mao B, He R and Hu J 2019 *Opt. Express* **27** 17729
[22] Akhmediev N, Soto-Crespo J M and Town G 2001 *Phys. Rev. E* **63** 056602
[23] Soto-Crespo J M, Akhmediev N and Ankiewicz A 2000 *Phys. Rev. Lett.* **85** 2937
[24] Yang S, Zhu Z, Qi Y, Jin L, Li L and Lin X 2023 *Chaos, Solitons and Fractals* **172** 113544
[25] Zhang Z X, Luo M, Chen J X, Chen L H, Liu M, Luo A P, Xu W C and Luo Z C 2022 *Opt. Lett.* **47** 1750
[26] Latas S C V and Ferreira M F S 2011 *Opt. Lett.* **36** 3085
[27] Latas S C V and Ferreira M F S 2010 *Opt. Lett.* **35** 1771

[28] Song L J, Li L, Li Z G and Zhou G S 2005 *Opt. Commun.* **249** 301
[29] Crasovan L C, Malomed B A and Mihalache D 2001 *Phys. Lett. A* **289** 59
[30] Shen H, Zhou R and Zhang Z 2024 *Chaos, Solitons and Fractals* **185** 115110
[31] He C, Zhu Z, Yang S, Wang N, Yang Y and Lin X 2024 *Opt. Express* **32** 11895
[32] Zhu Z, Yang S, He C and Lin X 2023 *Opt. Express* **31** 35529
[33] Blanco-Redondo A, Martijn d S C, Sipe J E, Krauss T F, Eggleton B J and Husko C 2016 *Nat. Commun.* **7** 10427
[34] Runge A F J, Hudson D D, Tam K K K, de Sterke C M and Blanco-Redondo A 2020 *Nat. Photon.* **14** 492
[35] Zhang Z X, Luo M, Liu J H, Yang Y T, Li T J, Liu M, Luo A P, Xu W C and Luo Z C 2024 *Nat. Commun.* **15** 6148
[36] Han Y, Gao B, Wu G, Huo J Y, Wen H L, Li Y Y, Liu L and Ma C Y 2023 *Opt. Express* **31** 1787
[37] Shen H Y, Lan R B, Hu H B, Li Y, Zhou R and Zhang Z X 2025 *Chin. Phys. B* **34** 034203
[38] Yao X, Liu C, Yang Z Y and Yang W L 2022 *Phys. Rev. Res.* **4** 013246
[39] Li Y, Xia R, Liu J, Zhao Y, Li C, Wang M, Zhang R, Tang X and Xu G 2024 *Opt. Laser Technol.* **175** 110900
[40] Wu Z L, Zang Z X, Li T J, Luo M, Liu M, Luo A P, Xu W C and Luo Z C 2025 *Opt. Express* **33** 10129
[41] Yang S, Zhu Z, Qi Y, Jin L, Li L and Lin X 2023 *Chaos Solitons and Fractals* **172** 113544
[42] Liu C, Che W J and Akhmediev N 2024 *Phys. Rev. E* **110** 044210
[43] Chen H J, Tan Y J, Long J G, Chen W C, Hong W Y, Cui H, Luo A P, Luo Z C and Xu W C 2019 *Opt. Express* **27** 28507